A Genetic Algorithm Optimized Fractal Model to Predict the Constriction Resistance from Surface Roughness Measurements

Francesca Capelli[1,2], Jordi-Roger Riba[1]*, Elisa Rupérez[1] and Josep Sanllehí[2]
[1]Universitat Politècnica de Catalunya, 08222 Terrassa, Barcelona, Spain
[2]SBI Connectors Spain, 08635 Sant Esteve Sesrovires, Barcelona. España, Spain
*Corresponding author. Tel. +34 937398365 e-mail: riba@ee.upc.edu

Abstract— The electrical contact resistance greatly influences the thermal behavior of substation connectors and other electrical equipment. During the design stage of such electrical devices it is essential to accurately predict the contact resistance to achieve an optimal thermal behavior, thus ensuring contact stability and extended service life. This paper develops a genetic algorithm (GA) approach to determine the optimal values of the parameters of a fractal model of rough surfaces to accurately predict the measured value of the surface roughness. This GA-optimized fractal model provides an accurate prediction of the contact resistance when the electrical and mechanical properties of the contacting materials, surface roughness, contact pressure and apparent area of contact are known. Experimental results corroborate the usefulness and accuracy of the proposed approach. Although the proposed model has been validated for substation connectors, it can also be applied in the design stage of many other electrical equipment.

Keywords—contact resistance, connectors, genetic algorithms, fractals, rough surfaces.

1. INTRODUCTION

The contact resistance is a fundamental parameter that greatly influences the efficiency, long-term service and stable performance of electrical connections. This paper analyzes the electrical contact resistance of substation connectors. The contact resistance of aluminum substation connectors can be much higher than the bulk resistance of the connector [1]. Such connectors have two parts which are mechanically tightened by means of bolts and nuts. Therefore a specified torque is applied to ensure connection integrity and a suitable contact resistance between the conductor or bus bar and the connector. During the design step of such electrical devices, it is of paramount importance to have a tool to accurately predict the contact resistance. As a result the correct thermal behavior can be ensured and optimized, otherwise the thermal stress tends to increment the contact resistance, thus increasing power losses and affecting contact stability and the expected service life [2].

Since the contact interface restricts the current carrying capacity of any electrical connection [3], it is of

paramount importance to develop accurate and reliable models to determine the electrical contact resistance to design optimized and competitive connectors and other electrical devices, this being a challenging problem [4]. The electrical contact resistance has two main components. The first term, known as electrical constriction resistance (ECR), is due to the roughness of the contacting surfaces since the electrical current has to flow through the geometric constriction. The second term, known as film resistance, is attributed to poorly conductive films or oxides formed at the contacts' interface [5]. In this work this latter term is almost removed by applying a previous chemical cleaning of the interface so that the main term of the contact resistance is the constriction resistance. The restriction resistance is greatly influenced by different variables such as the applied mechanical load, mechanical and electrical properties of the surfaces in contact or environmental conditions [6].

Early studies were pioneered by Holm [7] and Greenwood [8], who proposed analytical formulas to calculate the ECR due to round shaped clusters [5]. Different approaches to model the contact resistance of rough surfaces are found in the technical literature, including statistical, multiscale and fractal models [9]. Rough contact surfaces form multiple microscopic contact points tend to form clusters defining a real contact area within the apparent or macroscopic contact area [10]. Leidner *et al.* [3] concluded that the current distribution across the contact interface of two spherical surfaces is highly influenced by the surface roughness and observed a steady increase of the maximum current density when increasing the surface roughness, which was attributed to a decreasing number of contact spots.

Surface measurements have revealed that peaks and valleys associated to rough surfaces show a multiscale pattern [5], [11] with no evident smallest scale [10]. Fractal-based models are good candidates to reproduce constrictive effects taking into account such different scales [5], since most of the statistical models do not consider this phenomenon [9]. It is expected that when increasing the number of scales, the ECR approaches a limit value even under the elastic approach in which the real contact area is assumed to be proportional to the mechanical load intensity [5]. However, when considering a perfect fractal surface with infinite scales, the true area of contact comprises an infinite number of infinitely small contact spots, which are subjected to an infinite contact pressure [12]. According to Kwak *et al.* [10] and Wilson *et al.* [9], at sufficiently small scale, asperities deform plastically because the mechanical load intensity exceeds the critical value, and the areas of contact tend to group into clusters. Compared to pure elastic contacts, the pressure in elastic-plastic contacts decreases at the peak points and increases at the valleys, the plastic flow flattening the surface roughness [12]. The number of microcontact clusters determines the real contact area, their distribution being severely influenced by the small-scale surface roughness whereas their locations are determined by the large scale surface waviness. The ECR depends upon both the size and number of

microcontacts and their grouping into clusters [10].

Due to its random and multiscale nature, an accurate prediction of the ECR of rough surfaces is still a challenging problem [5]. Kogut and Kompoupoulos [13] developed a model to determine the contact resistance of conductive rough surfaces, assuming a fractal geometry, elastic-plastic asperities and size-dependent micro-contacts. However, fractal models are based on several variables whose values need to be tuned for each particular application. The tuning of these parameters is not a trivial task, so an automatic optimization system to perform this operation is highly desirable, which is one of the main contributions of this paper.

In the technical literature there is a lack of works dealing with the optimization problem of fractal models, although different studies analyze the relationship between the fractal dimension and different physical properties [14], [15] but with no optimization perspective. In [16], the fractal dimension D of two-dimensional rock joint profiles was estimated by formulating a classification problem and applying the PSO (particle swarm optimization) algorithm in combination with two multi-layer NNs (neural networks). However, this hybrid approach requires an exchange of information between the PSO and the NNs, and only estimates the fractal dimension D, although the roughness of the fractal profiles depends on other fractal parameters. In [17] and [18], the optimal fractal dimension of two manufactured surfaces was obtained by calculating the partial derivative of the normalized wear rate with respect to the fractal dimension of an empirical wear model, the accuracy of which greatly determines the precision of the optimal value of D. Moreover, the aim of this work is to estimate three surface parameters D, G and γ defined in Section 3, whereas most of the methods found in the technical literature are developed to only estimate the fractal dimension D, thus making a contribution in this field. A GA-based approach provides several advantages over the deterministic approach. GAs are suitable to solve either unconstrained and constrained optimization problems [19] in which the objective function can be single- or multi-objective. Moreover, these methods can be employed when the objective function is not linear and the input variables contain noise or are stochastic.

Different heuristic optimization (HO) methods have been developed to solve optimization problems that otherwise would be impossible or difficult to solve [20]. They share common features since they start off with a random initial solution, iteratively generate and evaluate new solutions based on an established generation rule and finally report the best solution attained [21]. The iterative search process is often halted when the error is below a predetermined threshold value, when there is no further solution improvement after a predetermined number of iterations or when the CPU time exceeds an imposed value. Among them different tools highlight, such as evolutionary computation, differential evolution, particle swarm, simulated annealing, ant colony systems, tabu search or memetic algorithms among others [20], [21].

Heuristic approaches are applied to solve a wide range of problems in many physical applications, including the control field in electromechanical [22], [23] and electrohydraulic systems [24] or to predict software quality attributes [25] among others. These tools offer major advantages including shorter development time compared to traditional approaches, and robustness since they are quite insensitive to missing data and noise. However, they present some disadvantages since the solution attained can be suboptimal and the application of such methods require trained and skilled users because previous experience and knowledge are fundamental.

This paper proposes a genetic algorithm (GA) approach to determine the optimal values of the parameters in the fractal model to accurately fit the measured surface roughness with that predicted by the fractal model of rough surfaces. GAs offer several advantages compared to other optimization methods, since they do not require an initial approximation of the solution, can handle with discontinuous and non-linear objective functions, allow seeking for multiple local optima [26] and use and operate a set of candidate solutions rather than refining a single-candidate solution as done by other optimizers. The classical optimizers have difficulties to solve global optimization nonlinear problems. This work deals with GA since, due to its random nature, the chances of finding a global optimum solution are enhanced with a reasonable computational time using a standard computer, which are among the main difficulties of this work. GA does not require the objective function to be continuous or differentiable, and allows solving general optimization problems, bound-constrained or unconstrained [27].

The goal of this work is to develop a GA-based approach to estimate, from simple and inexpensive surface roughness measurements, the values of three fractal parameters (D, G and γ defined in Section 3) of the contacting surfaces in an automatic, fast and effective manner to characterize the fractal surface features of the analyzed joint to accurately predict the constriction resistance. This is a challenging problem so far not well developed in the technical literature.The proposed surface roughness measurement can be done using an inexpensive stylus-type surface roughness tester which is available in many industry laboratories. Therefore, from the fractal model of the rough surface a reliable and accurate prediction of the ECR can be done if the mechanical and electrical properties of the interface materials, surface roughness, apparent area of contact and contact pressure are known. The proposed model allows predicting the contact resistance of electrical devices not yet manufactured, that is, during the design stage. Although this paper focuses on the calculation of the contact resistance of substation connectors during the design stage, the proposed approach can be applied to many other electrical devices with electrical contacts.

The following sections are organized as follows. Section 2 describes the parameters used to characterize the surface roughness. Section 3 develops the proposed GA-optimized fractal model. In Section 4 reference ECR models are explained for comparison purposes, Section 5 details the ECR measurements performed,

Section 6 compares the results obtained from the analyzed ECR models with measured values of three aluminum substation connectors and Section 7 develops the main conclusions of the paper.

2. SURFACE ROUGHNESS PARAMETERS

This section describes the main indexes used to characterize surface roughness according to the EN-ISO 4287 international standard [28]. The average value of the absolute roughness R_a (m) is defined as,

$$R_a = \frac{1}{n}\sum_{i=1}^{n}\left|z_i\right| \tag{1}$$

n being the number of points considered within the sampling length L, and z_i the roughness height value at point i-th.

The root-mean-square roughness R_q (m) is calculated as,

$$R_q = \sqrt{\frac{1}{n}\sum_{i=1}^{n} z_i^2} \tag{2}$$

Many ECR models for rough surfaces are based on the measurement of R_q. However, many simple surface roughness testers do not perform a direct measure of R_q and thus it is estimated from the experimental value of R_a. These testers usually assume idealized asperities exhibiting a full-wave rectified sinewave shape, thus R_q can be determined from R_a as [29], [30],

$$R_q = 1.11 \cdot R_a \tag{3}$$

However, when dealing with rough surfaces with asperities exhibiting a Gaussian distribution, the relationship between R_q and R_a can be expressed as [31],

$$R_q = \sqrt{\pi/2} \cdot R_a \cong 1.25 R_a \tag{4}$$

The relationship between R_q and R_a depends on the geometric distribution of the asperities, so the application of (3) and (4) can lead to inaccurate results, although these correlations are often required to estimate R_q and, therefore, to use most of the ECR models for rough surfaces found in the technical literature.

Other important roughness-related parameters are the maximum height of the profile, R_y and the average maximum height of the profile, R_z, which is defined as the average of the ten greatest peak-to-valley deviations in the evaluation length,

$$R_y = R_p - R_v \tag{5}$$

where R_p is the maximum peak height and R_v the maximum valley depth.

The average maximum height of the profile R_z is calculated as,

$$R_z = \frac{1}{10}\sum_{i=1}^{10}(R_{pi} - R_{vi}) \tag{6}$$

where R_{pi} and R_{vi} are, respectively, the *i-th* highest peak, and the *i-th* lowest valley.

To predict the ECR from the GA-optimized fractal model proposed in this work, a previous calculation of the surface roughness parameters by applying (1), (5) and (6) is required, as detailed in Section 3.

The dimensionless mean and root-mean square slopes, m_a and m_q respectively, are other parameters used to characterize the morphology of the asperities,

$$m_a = \frac{1}{n}\sum_{i=1}^{n}\left|\frac{dz_i}{dx}\right| \tag{7}$$

$$m_q = \sqrt{\frac{1}{n}\sum_{i=1}^{n}\left(\frac{dz_i}{dx}\right)^2} \tag{8}$$

However, an accurate measure of m_a or m_q requires complex instruments which are expensive and habitually not available. Therefore m_a is often approximated by applying different empirical correlations as $m_a = x\cdot(R_q)^y$, where x and y are parameters whose values depend on the bibliographic reference considered [32]–[34].

It is noted that R_a, R_z and R_y are the input variables of the GA-optimized fractal model proposed in this paper, as it will be fully described in Section 3, whereas, R_q and m_a are required in other recognized ECR models which are summarized in Section 4 to validate the proposed approach.

3. THE GA-OPTIMIZED FRACTAL MODEL

Mathematical methods accounting for multiscale effects, such as fractal-based methods, can provide a detailed description of the ECR and thus accurate solutions. Fractal methods are also appealing because allow dealing with multiscale topographies since they exhibit scale invariance features, so measurements are independent of sample length and instrument resolution [13]. In a fractal process, a portion of such process is the downscaled version of the whole [35]. The fractal-based ECR theory developed by Kogut and Komvopoulos (KK) [13] assumes a fractal geometry to describe the surface topography, elastic-plastic deformation of the interfacial asperities, and size-dependent ECR of the microcontacts in the real contact area. The KK fractal model applies a fractal approach to describe the roughness of a contact interface by means of scale-invariant parameters. The three-dimensional KK surface topography is generated by means of a truncated two-variable Weierstrass-Mandelbrot function,

$$z(x,y) = L\left(\frac{G}{L}\right)^{D-2}\left(\frac{\ln\gamma}{M}\right)^{0.5}\sum_{m=1}^{M}\sum_{n=0}^{n_{\max}}\gamma^{(D-3)n}\left(\cos\varphi_{m,n} - \cos A\right) \tag{9}$$

where A can be expressed as,

$$A = \left\{\frac{2\cdot\pi\cdot\gamma^n\left(x^2+y^2\right)^{0.5}}{L}\cos\left[\tan^{-1}\left(\frac{y}{x}\right) - \frac{\pi\cdot m}{M}\right] + \varphi_{m,n}\right\} \tag{10}$$

(x,y) being the surface points considered, $z(x,y)$ the elevation coordinate of such points, L the sampling length, D ($2 < D < 3$) the fractal dimension, G the fractal roughness, $\gamma > 1$ a scaling parameter, M the number of superposed ridges applied to generate the surface profile, n the frequency index with n_{max} the upper limit of n, and $\varphi_{m,n}$ ($0 < \varphi_{m,n} < 2\pi$) a random phase angle. The fractal dimension D is a measure of the complexity of the fractal pattern, thus quantifying the weight of the high-frequency components.

Once the fractal surface is generated, the roughness parameters R_a, $R$and R_z can be calculated by applying (1), (5) and (6), as shown in Fig. 1.

It is noted that in the following paragraphs some of the parameters are normalized with respect to the apparent contact area A_a, thus resulting in dimensionless parameters that are marked with an asterisk.

When $r < \lambda$, λ being the average mean free path of the electrons in the contacting materials, that is, $\lambda = (\lambda_1 + \lambda_2)/2$, and r the radius of the apparent area of contact A_a, it is assumed that the electrons pass across the contact area without scattering, so the constriction resistance is dominated by the Sharvin mechanism**.** Alternatively, when $r > \lambda$, the constriction resistance is dominated by the scattering of electrons across the contact area and thus by the Holm mechanism [13].

When dealing with cast aluminum substation connectors, the radius r of the apparent area of contact A_a is of the order of micrometers ($r \approx 10^{-6}$ m), whereas the mean free path of the electrons for aluminum can vary from some tens to several hundred angstroms ($\lambda \approx 10^{-9} - 3 \cdot 10^{-8}$ m), depending on their energy level [36]. Therefore, the second condition ($r > \lambda$) is fulfilled and the ECR is dominated by the Holm mechanism. According to the KK formulation, the ECR based on the Holm formulation [37] is calculated as the sum of individual parallel resistances corresponding to the constriction resistances of the contact points established during the installation of the electrical connection.

In the proposed GA-optimized model, the ECR is related to the Holm electrical conductivity C_H (Ω^{-1}) as,

$$ECR = 1/C_H \tag{11}$$

where

$$C_H = \frac{C_H^* \cdot A_a^{1/2}}{\rho_1 + \rho_2} \tag{12}$$

ρ_1 and ρ_2 being, respectively, the electrical resistivity of the connector and conductor surfaces in contact and A_a the apparent area of contact.

The dimensionless Holm electrical conductivity C_H* is calculated as follows,

$$C_H^* = \frac{2\sqrt{2}}{\sqrt{\pi}} \left(\frac{D-1}{D-2} \right) \cdot (a'_L{}^*)^{0.5} \cdot B \tag{13}$$

where

$$B = \sqrt{2}\left(\frac{a'_L{}^*}{a'_S{}^*}\right)^{\frac{D-2}{2}} - \left(\sqrt{2}-1\right)\left(\frac{a'_L{}^*}{a'_C{}^*}\right)^{\frac{D-2}{2}} - 1 \tag{14}$$

$a'_S{}^* = a'_S/A_a$ and $a'_C{}^* = a'_C/A_a$ being, respectively, the smallest dimensionless truncated microcontact area and the critical dimensionless truncated microcontact area and A_a the apparent area of contact. They set the threshold value between elastic and fully plastic deformation areas. When the area of the asperities accomplishes $a' > a'_C$, the asperities experiment an elastic deformation whereas when $a' < a'_C$ they experiment a fully plastic deformation. The dimensionless critical truncated micro-contact area $a'_C{}^*$ is defined as:

$$a'_C{}^* = \frac{a'_C}{A_a} = \frac{\left(2^{(9-2D)}\pi^{(D-2)}b^{-1}G^{(2D-4)}\left(\frac{E}{KY}\right)^2 \ln\gamma\right)^{1/(D-2)}}{A_a} \tag{15}$$

where $b = [0.5\cdot\pi\cdot(0.454 + 0.41\nu_1)]^2$, ν_1 being the Poisson's ratio of the softer material in the electrical connection and E ($N\cdot m^{-2}$) the reduced elastic modulus given by,

$$E = [(1 - \nu_1{}^2)/E_1 + (1 - \nu_2{}^2)/E_2]^{-1} \tag{16}$$

Subscripts 1 and 2 referring respectively, to the softer and harder material, Y (N/m^2) being the yield strength and $K = HB/Y$ the dimensionless ratio of the hardness to the corresponding yield strength.

The value of the largest truncated microcontact area $a'_L{}^*$, can be found by solving the implicit equation of the dimensionless contact pressure $P^* = P/(A_a\cdot E)$,

$$P^* = \frac{KY}{E}\left(\frac{D-1}{3-D}\right)a'_L{}^*\left[\left(\frac{a'_C{}^*}{a'_L{}^*}\right)^{(3-D)/2} - \left(\frac{a'_S{}^*}{a'_L{}^*}\right)^{(3-D)/2}\right] + p \tag{17}$$

P ($N\cdot m^{-2}$) being the contact pressure and,

$$p = \left[1 - \left(\frac{a'_C{}^*}{a'_L{}^*}\right)^{(5-2D)/2} + 1\right]\cdot\frac{2^{(11-2D)/2}}{3\pi^{(4-D)/2}}\left(\frac{D-1}{5-2D}\right)\cdot(\ln\gamma)^{0.5}G^{*(D-2)}\,(a'_L{}^*)^{(4-D)/2} \tag{18}$$

It is noted that the only unknown variable in (17) is $a'_L{}^*$, so it can be solved by applying the Newton-Raphson method.

The truncated two-variable Weierstrass-Mandelbrot fractal function in (9) includes different parameters (L, G, D, M, γ and n_{max}) that must be tuned to generate a three-dimensional geometry with a surface roughness similar to that of the real contact interface. The selection of the optimal values of such parameters to accurately reproduce the real rough surface requires the application of specific optimization tools. Since parameters L (sample length), L_o (cutoff length) and L_s (smallest characteristic length) can be selected beforehand for the specific application, they are assumed as constant values during the optimization process. For consistency, it is suggested to consider values of L almost 20 times the highest value of the measured arithmetical mean roughness R_a of the two contacting interfaces. The number of

ridges M to be superposed to generate the fractal surface can be determined as [38],

$$M = round(\log_{10}(L/L_o)/\log_{10}\gamma) \tag{19}$$

L_o being the smallest characteristic length which is in the order of equilibrium atomic distance, that is $L_o \approx 0.5$ nm and *round* being an operator that rounds to the nearest integer number.

According to [13], [38], the upper limit n_{max} of the frequency index n can be calculated as,

$$n_{max} = round[\log_{10}(L/L_s)/\log\ \gamma] \tag{20}$$

L_s being the lower cutoff corresponding to the size of individual particles [39], usually considered of about the material's interatomic distance [40].

In this paper the optimal values of the parameters G, D, M, γ and n_{max} are determined by the genetic algorithm. Only parameters G, D and γ are changed at each iteration by applying the GA rules, since L is considered as a constant value and parameters M and n_{max} are calculated from (19) and (20), respectively. The three-dimensional surface topography is iteratively generated from (9) and the values of the parameters L, G, D, M, γ and n_{max} are explored by the genetic algorithm. Next, at each iteration, the surface roughness parameters R_a, R_y and R_z are evaluated by applying (1), (5) and (6) for each fractal surface obtained. To reduce the inherent variability due to the random nature of (9), the fractal surface is generated three times at each iteration, and the average values of the R_a, R_y and R_z roughness parameters are calculated. Then an error or objective function is evaluated by comparing the calculated values of R_a, R_y and R_z with those obtained from experimental measurements (R_{a_meas}, R_{y_meas} and R_{z_meas}). The selected objective function to be minimized by the GA is as follows,

$$\varepsilon = \left(1 - \frac{R_a}{R_{a\_meas}}\right)^2 + \left(1 - \frac{R_y}{R_{y\_meas}}\right)^2 + \left(1 - \frac{R_z}{R_{z\_meas}}\right)^2 \tag{21}$$

Note that (21) evaluates the quadratic difference between the values of R_a, R_y and R_z calculated from the fractal surface generated from (9) and those measured by means of a surface roughness tester, that is, R_{a_meas}, R_{y_meas} and R_{z_meas}.

This iterative approach is applied until the error ε is below a certain threshold value as shown in Fig. 1. The iterative GA-based approach shown in Fig. 1, which applies a multi-start strategy, jointly with the imposed tolerance threshold, ensure to find an optimal solution.

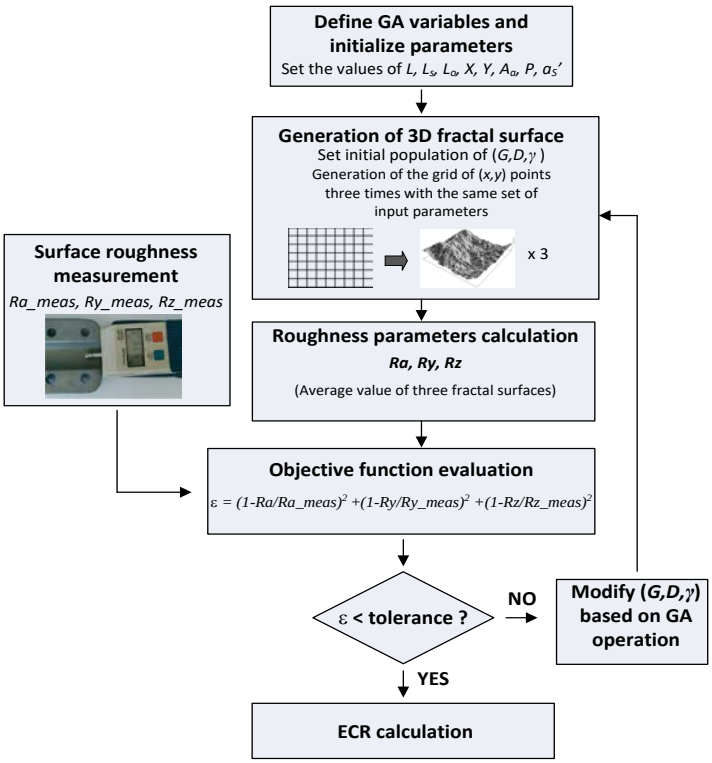

Fig. 1. GA-based optimized fractal model of the ECR

The GA is a heuristic search method applied to solve complex optimization problems [34] based on the laws of genetics and natural selection [35]. A population of 30 individuals R_a, R_y and R_z was considered, and a value encoding was used for the individuals, which are considered as real numbers. A scattered crossover was applied, a stochastic uniform function was chosen to perform the parent selection and a Gaussian mutation was selected. The stopping criteria were based on a function tolerance of 10^{-6} and a time limit of 3600 s.

The analyzed substation connectors have two identical contact areas as indicated in Fig. 2 and therefore the ECR must be calculated as,

$$ECR = \frac{1}{C_H} + \frac{1}{C_H} = \frac{2}{C_H} \tag{22}$$

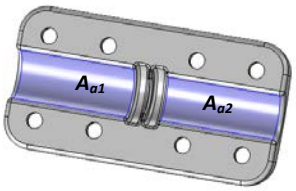

Fig. 2. Contact interfaces ($A_{a1} = A_{a2} = A_a$) between the conductors and the substation connector.

The optimization problem to be solved is based on determining the optimal values of the parameters in the fractal model (G, D and γ) to accurately match the measured values of the surface roughness with those calculated by the fractal model by means of (1), (5), (6) and (22).

4. REFERENCE ECR MODELS

This section describes the HG (Holm-Greenwood) and CMY (Cooper, Mikic and Yovanovich) models, which are widely applied in the technical literature and used as reference models for accuracy comparison purposes.

4.1 Holm-Greenwood model

Holm theory of smooth contacts [7] has pioneered ECR models. It assumes that the electrical current across rough contact surfaces flows through circular a-spots (small circular spots). According to the Holm model, the constriction of the current paths through the a-spots generates the ECR. Greenwood realized that the asperities are often grouped forming clusters [41], [42] and improved the Holm's model by adding an additional term to the ECR equation to account for the clusters effects. According to the HG (Holm-Greenwood) model, the ECR can be calculated as,

$$ECR = \rho\left(\frac{1}{2na} + \frac{1}{2\alpha}\right) \tag{23}$$

ρ being the electrical resistivity of the contacting surfaces, n the number of a-spots, a the radius of the a-spots and α the cluster radius. It is noted that the first term in (23) is due to Holm whereas the second term was added by Greenwood. To calculate (23) the values of parameters n, a and α are required, although this information is often difficult to obtain. According to [43], the ECR of a fixed area interface is independent of the number and geometrical distribution of the a-spots. This means that the first term in (23) is negligible compared to the second term. Therefore by only knowing the cluster radius α, it is possible to predict the ECR. The real area of contact A_c (m^2) is related to the mechanical load F (N) and the plastic flow stress H (N/m^2) as,

$$A_c = F/H \tag{24}$$

The cluster radius α can be inferred from the real area of contact as

$$\alpha = \sqrt{A_c / \pi} \tag{25}$$

Finally, the ECR can be obtained as follows,

$$ECR = \frac{\rho}{2\alpha} = \sqrt{\frac{\rho^2 \pi H}{4F}} \tag{26}$$

Due its simplicity, (26) has been widely used in the area of instrumentation and measurement [44]. Since (26) does not consider effects such as surface roughness or the apparent area of contact, its accuracy is expected to be limited. For example, when analyzing substation connectors with different geometries and, thus, different apparent contact areas, the results predicted by (26) will be the same, which seems no realistic.

4.2 CMY Model

Cooper, Mikic and Yovanovich (CMY) developed a statistical thermal model for the contact resistance of rough surfaces [45] which was improved in later works [46]–[49]. This model can also be applied to the analysis of electrical contacts because of the close similarity between the thermal and the electric models [50]. The CMY model of the ECR assumes that asperities in the contact interface present a peaks-valleys Gaussian distribution and are randomly distributed across the apparent area of contact [45]. The CMY model assumes isotropic rough surfaces and plastic deformation of the interfacial asperities. The ECR (Ω) is calculated as,

$$ECR = A_a \cdot \left(1.25 \frac{1}{\rho_{joint}} \frac{m_{joint}}{Rq_{joint}} \cdot (p_{rel})^{0.95} \right)^{-1} \tag{27}$$

The electrical resistivity of the joint ρ_{joint} ($\Omega^{-1} \cdot m^{-1}$) is calculated as,

$$\rho_{joint} = (\rho_1 + \rho_2)/2 \tag{28}$$

ρ_1 and ρ_2 being the electrical resistivity of the two contacting surfaces. R_q and m_a are the root-mean-square roughness and the asperity slope for the interface formed by the two rough surfaces in contact, which can be calculated as [45],

$$R_{q,joint} = \sqrt{R_{q1}^{\ 2} + R_{q2}^{\ 2}} \tag{29}$$

$$m_{a,joint} = \sqrt{m_{a1}^{\ 2} + m_{a2}^{\ 2}} \tag{30}$$

subscripts 1 and 2 denoting both contacting surfaces.

The dimensionless relative pressure p_{rel} at the interface is calculated as [45],

$$p_{rel} = \left(P / [c_1 \left(1.62 \cdot \frac{R_{q,joint}}{R_{q,0}} \cdot m_{a,joint} \right)^{c_2}] \right)^{1/(1+0.071 \cdot c_2)} \tag{31}$$

$m_{a,joint}$ being the average slope of the asperities in the joint, P the contact pressure ($N \cdot m^{-2}$), $R_{q,0}$ = 1 µm, H_0 = 3178 MPa and parameters c_1 ($N \cdot m^{-2}$) and c_2 (dimensionless) are calculated from the Brinell hardness H_B ($N \cdot m^{-2}$) of the softer material as [45],

$$c_1 = \left(4.0 - 5.77 \frac{H_B}{H_0} + 4.0 \left(\frac{H_B}{H_0} \right)^2 - 0.61 \left(\frac{H_B}{H_0} \right)^3 \right) \cdot H_0 \tag{32}$$

$$c_2 = 0.37 + 0.442 \frac{H_B}{c_1} \tag{33}$$

However, the CMY estimation of the ECR given by (27) depends on the slope $m_{a,joint}$. Although it can be measured by using three-dimensional optical profilers or laser interferometers, they are expensive and scarcely found in industrial environments, thus limiting their applicability in numerous industry applications. Another possibility is the estimation of $m_{a,joint}$ from the measured values of the surface

roughness, but this estimation is often inaccurate [51] when applying the approximations found in the literature [32]–[34]. These shortcomings in the measurement or estimation of $m_{a,joint}$ limit the applicability of the CMY model.

5. SURFACE ROUGHNESS AND ECR MEASUREMENT

Three types of substation connectors from the catalogue of SBI Connectors and AAAC (All Aluminum Alloy Conductor) conductors (SALCA 593, 32 mm diameter) are studied, which are shown in Fig. 3. The studied substation connectors are made of A356.0 aluminum alloy with T6 heat-treatment and the AAAC conductors of 1350 Al alloy.

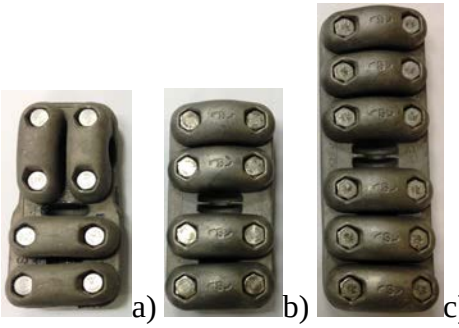
a) b) c)

Fig 3. Analyzed substation connectors. a) S330TLS T-type substation connector. b) S330SLS coupler connector. c) S330SNS coupler connector.

To minimize the film resistance due to the formation of a nanometric layer of alumina and to improve substation connectors' thermal performance, a chemical solution was applied to the contacting surfaces for 45 minutes [52]. Next, the contacting surfaces were cleaned and the connectors and conductors were assembled following the standard assembly procedure [53]. In a previous investigation [52] it has been shown that this surface treatment allows almost complete removal the alumina film formed at the contact interface, and thus of the film component of the contact resistance.

Surface roughness measurements can be achieved through different methods, the simpler one consisting in a mechanical stylus profiler, which is in contact with the surface being measured. Due to the peaks and valleys characterizing the surface, the tip of the profiler is raised and lowered from a reference point. The result provided from a stylus profiler is often expressed as a single parameter (R_a), although some models measure other surface roughness parameters. Although non-contact surface roughness measurement methods such as optical interferometry can provide better resolution and more information, they require expensive instruments and can be affected by the optical properties of the sample or by oil or grease films covering many metal components. The surface roughness of both the substation connectors and conductors dealt with was measured by using an inexpensive Mitutoyo Surftest 211 surface roughness tester, which provides fast measurements of the of R_a, R_y and R_z parameters according to the EN-ISO 4287 standard [28].

The ECR of the connector-conductor system was measured by means of a digital micro-ohm meter Raytech Micro-Centurion II, which provides a maximum output current of 200 A_{DC} and a measurement accuracy of ± 0.01μΩ. It is based on the 4-terminal measurement technique. The ECR was measured as,

$$ECR = R_{AB} - R_{cond} - R_{conn} \tag{34}$$

R_{AB} being the resistance measured between points *A* and *B* (see Fig. 4), R_{cond} the resistance of the portion of the conductor between terminals *A* and *B*, and R_{conn} the bulk resistance of the connector, which can be calculated from electromagnetic three-dimensional FEM (finite-element method) simulations. The resistance of the conductor was measured similarly, by using a conductor length of 1 m and the result was scaled proportionally to the length of the conductor between points *A* and *B*.

The axial force *F* at the contact interface has to be measured to determine the contact pressure *P* in (17) and (31) and the real area of contact A_c in (24). It was measured by means of the torque clamp test, using the same type of stainless steel bolts and nuts required to join the connectors and conductors analyzed in this paper. After applying a suitable torque to the M10 bolts (35 N·m), which was controlled by means of a calibrated HBM TB1A torque transducer, the axial force was measured by means of a SENSOTEC D/7080-07calibrated dynamometer.

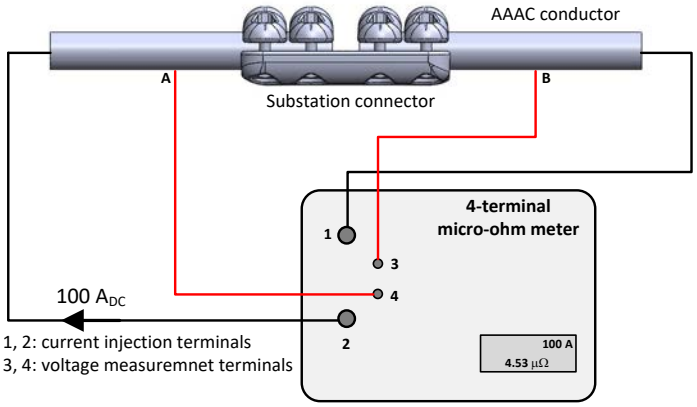

Fig 4. ECR measurement by using a micro-ohm meter based on the 4-terminal method [1].

6. RESULTS

In this section the ECR measurements of three analyzed aluminum substation connectors (S3300TLS, S3300SLS and S3300SNS shown in Fig. 5) are compared with the results obtained from the three different ECR models detailed in Sections 3 and 4.

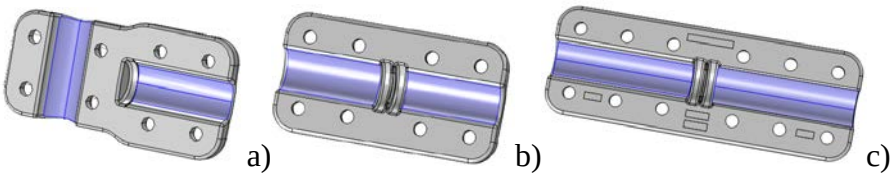

Fig 5. Apparent area of contact (in blue) in the three analyzed substation connectors a) S330TLS, b) S330SLS and c) S330SNS.

Table I summarizes the electrical and mechanical aluminum properties of the connectors and conductors required in the different ECR models.

TABLE I
ALUMINUM PROPERTIES [54]

Variable	Description	Value	Model
	Connector		
ρ_1	Electrical resistivity of Al alloy	$5.2 \cdot 10^{-8}$ Ω·m	HG-CMY-GA
v_1	Poisson's ratio of Al alloy	0.33	GA
E_1	Young modulus of Al alloy	70 GPa	GA
	Conductor		
ρ_2	Electrical resistivity of Al	$2.9 \cdot 10^{-8}$ Ω·m	HG-CMY-GA
v_2	Poisson's ratio of Al	0.33	GA
E_2	Young modulus of Al	70 GPa	GA
Y	Yield strength of Al	73 MPa	HG- GA
H	Plastic flow stress of Al	219 MPa	HG
HB	Brinell hardness of Al	150 MPa	CMY

Table I only provides information about *Y*, *H* and *HB* of the conductor material since it is the softer material in the contact.

Table II shows the parameters required to determine the ECR of the analyzed substation connectors and their values.

TABLE II
SUBSTATION CONNECTORS PARAMETERS

Variable	Description	Value	Model
$F_{,TLS}$ [1]	Contact axial force	4x15500 N	HG-CMY-GA
$F_{,SLS}$ [1]	Contact axial force	4x15500 N	HG-CMY-GA
$F_{,SNS}$ [2]	Contact axial force	6x15500 N	HG-CMY-GA
$Aa_{,TLS}$	Apparent area of contact (S3300TLS connector)	$2x29.5 \cdot 10^{-4}$ m^2	CMY-GA
$Aa_{,SLS}$	Apparent area of contact (S3300SLS connector)	$2x32.5 \cdot 10^{-4}$ m^2	CMY-GA
$Aa_{,SNS}$	Apparent area of contact (S3300SNS connector)	$2x49.5 \cdot 10^{-4}$ m^2	CMY-GA

[1] S330TLS and S330SLS connectors have four bolts in each contact interface

[2] S330SNS connector has six bolts in each contact interface.

The total axial force results from multiplying the axial force in each bolt by the number of bolts.

The apparent area of contact A_a indicated in Fig. 5, was calculated using a 3D-CAD software. The two contact areas of the three analyzed connectors are identical, and thus $A_{a1} = A_{a2} = A_a$.

Table III summarizes the results of the surface roughness measurements obtained with the Mitutoyo Surftest 211 surface roughness tester.

TABLE III
SURFACE ROUGHNESS MEASUREMENTS

Variable	Description	Value	Model
Ra_{connec}	Arithmetical average roughness of the connector's surface[1]	4.08 μm	CMY-GA
Ra_{cond}	Arithmetical average roughness of the conductor's surface[1]	0.36 μm	CMY
Ry_{connec}	Maximum roughness height of the connector's surface	30.45 μm	GA
Rz_{connec}	Average maximum roughness[1] height of the connector's surface	28.30 μm	GA

[1]Average value of 15 measurements in different points of the analyzed surfaces

Table IV summarizes the parameters used to generate the three-dimensional fractal contact interfaces of the three analyzed models. The parameters G, D, M, γ and n_{max} were obtained from the GA optimization carried out according to the sequence detailed in Fig. 1.

TABLE IV
PARAMETERS USED IN THE GA FRACTAL MODEL

Variable	Description [13]	S3300TLS connector	S3300SLS connector	S3300SNS connector
G	Fractal roughness	$1.0427 \cdot 10^{-7}$	$6.5789 \cdot 10^{-8}$	$4.8985 \cdot 10^{-8}$
D	Fractal dimension	2.3194	2.3084	2.3012
γ	Scaling parameter	1.4030	1.4375	1.5433
M	Number of superposed ridges	36	30	45
n_{max}	Upper limit of the frequency index	27	25	21
-	Grid size	500x500	500x500	500x500
L	Sample length	0.1 mm	0.1 mm	0.1 mm
L_s	Cutoff length	10 nm	10 nm	10 nm
L_o	Smallest characteristic length	0.5 nm	0.5 nm	0.5 nm
a'_s	Smallest truncated microcontact area	$6 \cdot 4.5 \cdot 10^{-10}$ m	$6 \cdot 4.5 \cdot 10^{-10}$ m	$6 \cdot 4.5 \cdot 10^{-10}$ m

The smallest truncated microcontact area a'_S was estimated as six times the lattice dimension of the contacting material [55].

Fig. 6 shows the three-dimensional fractal surfaces of the contact interfaces obtained by applying (9) with L = 0.1 mm, L_s = 10 nm and a grid size of 500x500 points.

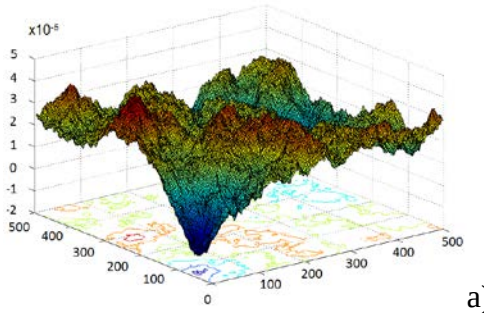

a)

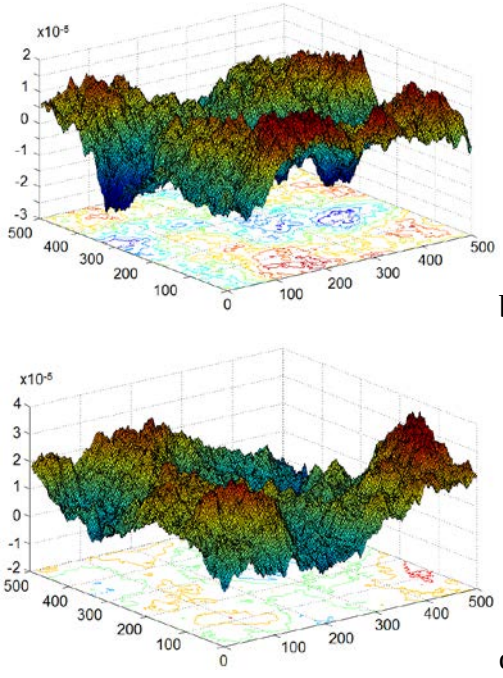

Fig. 6. Three-dimensional fractal surfaces of the contact interface of the analyzed substation connectors (100 μm x100 μm square section with a resolution of 500x500 points). a) S330TLS. b) S330SLS. c) S330SNS.

Table V summarizes the measured ECR values and those obtained by means of the GA-optimized fractal model proposed in this paper and the reference HG and CMY models. To account for the inherent dispersion among samples, the measured ECR values displayed in Table V are the average values of five specimens of each substation connector.

TABLE V
ECR RESULTS. MEASURED AND PREDICTED ECR VALUES FROM THE DIFFERENT ANALYZED MODELS

Substation connector	Measured values	GA-fractal Model	HG Model	CMY Model*
S330TLS	5.55 μΩ	5.54 μΩ	4.26 μΩ	3.57–7.67 μΩ
Difference		0.1%	23.2%	26.4–38.1%
S330SLS	5.26 μΩ	5.89 μΩ	4.26 μΩ	3.56–7.65 μΩ
Difference		11.9%	19.0%	26.0–45.4%
S330SNS	6.69 μΩ	6.53 μΩ	3.48 μΩ	2.37–5.10 μΩ
Difference		2.3%	47.9%	23.7–64.5%

*R_q calculated from (3) and (4) and m_a from [31], [33]

Results summarized in Table V show that the proposed GA-optimized fractal ECR model is the one providing better results when compared to experimental data. The error using the GA-fractal model is below 12% for all analyzed substation connectors. The error is 19-48 % for the HG model and 24-64% for the CMY model.

It can be concluded that experimental results validate the feasibility of the proposed GA-fractal model,

which allows obtaining accurate predictions of the ECR. It is also noted that results provided by both the HG (although it does not take into account the surface roughness and the apparent area of contact) and CMY models are of the same order of magnitude than measured values.

7. CONCLUSION

Substation connectors are designed for a service life of more than 30 years, and therefore it is mandatory to ensure a suitable thermal behavior. The contact resistance is one of the key factors determining the thermal performance of substation connectors and other electrical equipment. There is an imperious need to develop specific software tools to accurately predict the contact resistance of such electrical devices during the design phase, thus enabling to obtain more optimized products with an extended service life. To this end, this paper has developed a software tool based on a fractal model of the rough surfaces and a GA-based approach to determine the optimum values of the fractal model parameters to obtain an accurate prediction of the contact resistance from the measured values of the surface roughness, when the properties of the contacting materials, the contact pressure and the apparent area of contact are known. ECR estimations provided by the proposed GA-optimized fractal model have been compared with results provided by other internationally recognized ECR models, such as the Holm-Greenwood and the Cooper-Mikic-Yovanovich models. Experimental measurements performed on three typologies of substation connectors have proved a better accuracy of the ECR prediction provided by the GA-optimized fractal model. This experimental validation proves the suitability of the proposed model, which can be a valuable tool to assist the design and the optimization processes of substation connectors and other electrical equipment.

ACKNOWLEDGMENTS

The authors would like to thank SBI-Connectors Spain that supported this study by provisioning the samples and the equipment required for the experimental tests. They also thank the Spanish Ministry of Economy and Competitiveness and Generalitat de Catalunya for the financial support received under projects RTC-2014-2862-3 and DI-2013-024, respectively.

REFERENCES

[1] F. ; Capelli, J.-R. Riba, and D. Gonzalez, “Thermal behavior of energy-efficient substation connectors,” in *10th International Conference on Compatibility, Power Electronics and Power Engineering (CPE-POWERENG)*, 2016, pp. 104–109.

[2] F. Capelli, J.-R. Riba, and J. Pérez, “Three-Dimensional Finite-Element Analysis of the Short-Time

and Peak Withstand Current Tests in Substation Connectors,” *Energies*, vol. 9, no. 6, p. 418, May 2016.

[3] M. Leidner, H. Schmidt, and M. Myers, “Simulation of the Current Density Distribution within Electrical Contacts,” in *2010 Proceedings of the 56th IEEE Holm Conference on Electrical Contacts*, 2010, pp. 1–9.

[4] A. Bemporad and M. Paggi, “Optimization algorithms for the solution of the frictionless normal contact between rough surfaces,” *Int. J. Solids Struct.*, vol. 69, pp. 94–105, 2015.

[5] M. Ciavarella, G. Murolo, and G. Demelio, “The electrical/thermal conductance of rough surfaces—the Weierstrass–Archard multiscale model,” *Int. J. Solids Struct.*, vol. 41, pp. 4107–4120, 2004.

[6] C. Zhai, D. Hanaor, G. Proust, and Y. Gan, “Stress-Dependent Electrical Contact Resistance at Fractal Rough Surfaces,” *J. Eng. Mech.*, no. 5, p. B4015001, 2015.

[7] R. Holm, *Electric Contacts - Theory and Application Springer*. New York: Springer-Verlag, 1967.

[8] J. A. Greenwood and J. B. P. Williamson, “Contact of Nominally Flat Surfaces,” *Proc. R. Soc. A Math. Phys. Eng. Sci.*, vol. 295, no. 1442, pp. 300–319, Dec. 1966.

[9] W. E. Wilson, S. V. Angadi, and R. L. Jackson, “Surface separation and contact resistance considering sinusoidal elastic–plastic multi-scale rough surface contact,” *Wear*, vol. 268, no. 1–2, pp. 190–201, Jan. 2010.

[10] N. S. Noh Sung Kwak, J. Jongsoo Lee, and Y. H.-A.-B. C. of M. D. to M. E. C. R. Yong Hoon Jang, “Genetic-Algorithm-Based Controlling of Microcontact Distributions to Minimize Electrical Contact Resistance,” *IEEE Trans. Components, Packag. Manuf. Technol.*, vol. 2, no. 11, pp. 1768–1776, Nov. 2012.

[11] D. A. H. Hanaor, Y. Gan, and I. Einav, “Contact mechanics of fractal surfaces by spline assisted discretisation,” *Int. J. Solids Struct.*, vol. 59, pp. 121–131, 2015.

[12] Z. Wang, W. Wang, Y. Hu, and H. Wang, “A Simplified Numerical Elastic-Plastic Contact Model for Rough Surfaces,” in *Advanced Tribology*, Berlin, Heidelberg, Heidelberg: Springer Berlin Heidelberg, 2009, pp. 159–166.

[13] L. Kogut and K. Komvopoulos, “Electrical contact resistance theory for conductive rough surfaces,” *J. Appl. Phys.*, vol. 94, no. 5, p. 3153, Aug. 2003.

[14] X. Feng, L. Wei, and F. Lu, “Research on Relationship between Fractal Parameters and Compressive Stress of Metallic Gaskets,” in *2009 International Conference on Measuring Technology and Mechatronics Automation*, 2009, pp. 887–890.

[15] B. Li, R. Liu, and Y. Jiang, “A multiple fractal model for estimating permeability of dual-porosity media,” *J. Hydrol.*, vol. 540, pp. 659–669, 2016.

[16] N. Babanouri, S. Karimi Nasab, and S. Sarafrazi, “A hybrid particle swarm optimization and multi-layer perceptron algorithm for bivariate fractal analysis of rock fractures roughness,” *Int. J. Rock Mech. Min. Sci.*, vol. 60, pp. 66–74, 2013.

[17] G. Zhou, M. Leu, and D. Blackmore, “Fractal geometry modeling with applications in surface characterisation and wear prediction,” *Int. J. Mach. Tools Manuf.*, vol. 35, no. 2, pp. 203–209, Feb. 1995.

[18] H. Bin Liu, D. P. Wan, and D. J. Hu, “Fractal Characteristic and Wear Prediction of Surface Micro-Topography of Laser-Textured Roller,” *Key Eng. Mater.*, vol. 373–374, pp. 762–765, 2008.

[19] H. Saavedra, J.-R. Riba, and L. Romeral, “Multi-objective Optimal Design of a Five-Phase Fault-Tolerant Axial Flux PM Motor,” *Adv. Electr. Comput. Eng.*, vol. 15, no. 1, pp. 69–76, 2015.

[20] K. Y. Lee and M. A. El-Sharkawi, *Modern heuristic optimization techniques : theory and applications to power systems*. Wiley, 2008.

[21] D. G. Maringer, *Portfolio Management with Heuristic Optimization*, vol. 1. Berlin/Heidelberg: Springer-Verlag, 2005.

[22] D. MartÃ-n, B. Caballero, and R. Haber, “Optimal Tuning of a Networked Linear Controller Using a Multi-Objective Genetic Algorithm. Application to a Complex Electromechanical Process,” in *2008 3rd International Conference on Innovative Computing Information and Control*, 2008, pp. 91–91.

[23] R.-C. David, R.-E. Precup, E. M. Petriu, M.-B. Rădac, and S. Preitl, “Gravitational search algorithm-based design of fuzzy control systems with a reduced parametric sensitivity,” *Inf. Sci. (Ny).*, vol. 247, pp. 154–173, 2013.

[24] P. Mandal, R. Saha, S. Mookherjee, A. Chatterjee, and D. Sanyal, “Lessons learned from using some bio-inspired optimizers for real-time controller design for a low-cost electrohydraulic system,” *Appl. Soft Comput.*, vol. 48, pp. 638–649, 2016.

[25] D. Azar, K. Fayad, and C. Daoud, “A Combined Ant Colony Optimization and Simulated Annealing Algorithm to Assess Stability and Fault-Proneness of Classes Based on Internal Software Quality Attributes,” *Int. J. Artif. Intell.*, vol. 14, no. 2, pp. 137–156, 2016.

[26] C. Kwon and S. D. Sudhoff, “Genetic Algorithm-Based Induction Machine Characterization Procedure With Application to Maximum Torque Per Amp Control,” *IEEE Trans. Energy Convers.*, vol. 21, no. 2, pp. 405–415, Jun. 2006.

[27] P. Bajpai and K. Manoj, “Genetic algorithm – an approach to solve global optimization,” *Indian J. Comput. Sci. Eng.*, vol. 1, no. 3, pp. 199–206, 2010.

[28] ISO, “ISO 4287:1997 Geometrical Product Specifications (GPS) -- Surface texture: Profile method

-- Terms, definitions and surface texture parameters.” p. 25, 1997.

[29] A. A. Akbari, A. M. Fard, and A. G. Chegini, “An Effective Image Based Surface Roughness Estimation Approach Using Neural Network,” in *2006 World Automation Congress*, 2006, pp. 1–6.

[30] A. . Baker and W. . Giardini, “Developments in Australia’s surface roughness measurement system,” *Int. J. Mach. Tools Manuf.*, vol. 41, no. 13, pp. 2087–2093, 2001.

[31] F. F. Ling, “On Asperity Distributions of Metallic Surfaces,” *J. Appl. Phys.*, vol. 29, no. 8, p. 1168, Jun. 1958.

[32] L. H. Tanner and M. Fahoum, “A study of the surface parameters of ground and lapped metal surfaces, using specular and diffuse reflection of laser light,” *Wear*, vol. 36, no. 3, pp. 299–316, Mar. 1976.

[33] V. W. Antonetti, T. D. Whittle, and R. E. Simons, “An Approximate Thermal Contact Conductance Correlation,” *J. Electron. Packag.*, vol. 115, no. 1, p. 131, Mar. 1993.

[34] M. A. Lambert and L. S. Fletcher, “Thermal Contact Conductance of Spherical Rough Metals,” *J. Heat Transfer*, vol. 119, no. 4, p. 684, Nov. 1997.

[35] A. Maddahi, W. Kinsner, and N. Sepehri, “Internal Leakage Detection in Electrohydrostatic Actuators Using Multiscale Analysis of Experimental Data,” *IEEE Trans. Instrum. Meas.*, pp. 1–14, 2016.

[36] H. Kanter, “Slow-Electron Mean Free Paths in Aluminum, Silver, and Gold,” *Phys. Rev. B*, vol. 1, no. 2, pp. 522–536, Jan. 1970.

[37] R. Holm, *Electric Contacts*. Berlin, Heidelberg: Springer Berlin Heidelberg, 1967.

[38] A. Banerji, *Fractal Symmetry of Protein Exterior*. Pune, India: Springer Basel, 2013.

[39] C. G. Vayenas, R. E. White, and M. E. Gamboa-Aldeco, Eds., *Modern Aspects of Electrochemistry*, vol. 42. New York, NY: Springer New York, 2008.

[40] X. Yin and K. Komvopoulos, “An adhesive wear model of fractal surfaces in normal contact,” *Int. J. Solids Struct.*, vol. 47, no. 7, pp. 912–921, 2010.

[41] P. G. Slade, *Electrical Contacts*. CRC Press, 2014.

[42] J. A. Greenwood, “Constriction resistance and the real area of contact,” *Br. J. Appl. Phys.*, vol. 17, no. 12, pp. 1621–1632, Dec. 1966.

[43] M. Nakamura and I. Minowa, “Computer Simulation for the Conductance of a Contact Interface,” *IEEE Trans. Components, Hybrids, Manuf. Technol.*, vol. 9, no. 2, pp. 150–155, Jun. 1986.

[44] N. Kandalaft, I. I. Basith, and R. Rashidzadeh, “Low-Contact Resistance Probe Card Using MEMS Technology,” *IEEE Trans. Instrum. Meas.*, vol. 63, no. 12, pp. 2882–2889, Dec. 2014.

[45] M. G. Cooper, B. B. Mikic, and M. M. Yovanovich, “Thermal contact conductance,” *Int. J. Heat*

Mass Transf., vol. 12, no. 3, pp. 279–300, Mar. 1969.

[46] B. Mikic, “Analytical Studies of Contact of Nominally Flat Surfaces; Effect of Previous Loading,” *J. Lubr. Technol.*, vol. 93, no. 4, p. 451, Nov. 1971.

[47] B. B. Mikić, “Thermal contact conductance; theoretical considerations,” *Int. J. Heat Mass Transf.*, vol. 17, no. 2, pp. 205–214, Feb. 1974.

[48] M. M. Yovanovich, “Thermal contact correlations,” *Am. Inst. Aeronaut. Astronaut.*, pp. 83–95, 1982.

[49] M. M. Yovanovich, “Four decades of research on thermal contact, gap, and joint resistance in microelectronics,” *IEEE Trans. Components Packag. Technol.*, vol. 28, no. 2, pp. 182–206, Jun. 2005.

[50] G. Zavarise and D. Boso, “Electro-mechanical problems in superconductiong coils.” 05-Oct-2002.

[51] M. Bahrami, J. R. Culham, M. M. Yananovich, and G. E. Schneider, “Review of Thermal Joint Resistance Models for Nonconforming Rough Surfaces,” *Appl. Mech. Rev.*, vol. 59, no. 1, p. 1, Jan. 2006.

[52] F. Capelli, J.-R. Riba, A. Rodriguez, and S. Lalaouna, “Research towards Energy-Efficient Substation Connectors,” in *3rd International Congress on Energy Efficiency and Energy Related Materials*, 2016, pp. 295–301.

[53] Burndy, *Electrical Contacts: Principles and Applications*. 1999.

[54] J. R. Davis, *ASM Specialty Handbook: Aluminum and Aluminum Alloys - ASM International*. ASM International, 1993.

[55] K. Komvopoulos and N. Ye, “Three-Dimensional Contact Analysis of Elastic-Plastic Layered Media With Fractal Surface Topographies,” *J. Tribol.*, vol. 123, no. 3, p. 632, 2001.